ChemComm

COMMUNICATION

View Article Online
View Journal | View Issue

Cite this: *Chem. Commun.*, 2019, **55**, 1955

Received 31st December 2018,
Accepted 14th January 2019

DOI: 10.1039/c8cc10311a

rsc.li/chemcomm

NAG-targeting fluorescence based probe for precision diagnosis of kidney injury†

Fei Yan,‡[a] Xiangge Tian,‡[a] Zhilin Luan,[a] Lei Feng,*[abc] Xiaochi Ma *[a] and Tony D. James *[b]

We report an enzyme-activated fluorescence based probe (NHPO) for the selective detection of *N*-acetyl-β-D-glucosaminidase (NAG) activity in a drug-induced kidney injury mice model and NAG level in crude human urine. We used NHPO to explore the biological functions of NAG and provide a reference for the prognosis and prediction of proximal renal tubular dysfunction associated with various kidney diseases.

Chronic kidney disease (CKD), acute renal failure (ARF) and terminal-stage renal disease are common in hospitalized patients and increase the risks of morbidity and mortality. Most kidney injury is associated with complications of type 2 diabetes mellitus (DM)[1] or induced kidney injury by drugs[2] such as cisplatin.[3] Therefore, there is an urgent unmet need for the early diagnosis of both drug-induced kidney injury and that caused by disease complications such as diabetes mellitus, hypertension[4] *etc.* Over 20 biomarkers as an early clinical index of kidney injury have been studied both in blood and urine,[5] such as urinary albumin, neutrophil gelatinase-associated lipocalin (NGAL), interleukin-18 (IL-18), kidney injury molecule-1 (KIM-1) and liver-type fatty acid-binding protein. However, these biomarkers still face numerous challenges as clinical indicators for the diagnosis of renal injury due to difficult quantification and detection. The proximal tubule (PT) part of the kidney nephron, is a vital portion of the duct system that can efficiently regulate pH values of the urine by exchanging hydrogen ions in the interstitium for bicarbonate ions. It is also responsible for secreting organic acids, such as creatinine and other bases, into the urine filtrate. The proximal tubular epithelial cells (PTECs) participate in the progression of tubulointerstitial injury with a pivotal role in various kidney diseases. Therefore, it is essential to detect in real-time PTECs during the development and progression of kidney injury in a clinical environment.

N-Acetyl-β-D-glucosaminidase (NAG) has gained significant attention since its clinical implications in the sensitive detection and accurate prediction of kidney injury.[6] NAG is mainly distributed in the cytoplasm of the proximal tubular cell and plasma NAG cannot be filtered through the glomerulus due to its high molecular weight (130 kDa). However, during renal tubule injury, the proximal tubular cell exclusively secretes NAG resulting in a significant increase of NAG in the urine.[7]

A commercial assay kit has been developed to assay the NAG activity in the clinic using a colorimetric method.[8] However, in many cases this assay method is infeasible due to low sensitivity, significant background interference and laborious measurement procedure. Therefore, it is essential to develop an effective method for real-time NAG activity monitoring in complex biological systems. Over recent years fluorescent probes have received considerable attention for rapid and sensitive diseases diagnosis due to their numerous advantages, such as high sensitivity, real-time detection, high spatiotemporal resolution, non-invasive monitoring and use in living systems.[9] Relatively few fluorescent probes had been developed for the detection of NAG in tumours.[10] Additionally, a fluorescence based NAG assay for precision diagnosis of kidney injury is not currently available.

In our current research, we developed an enzyme-activated fluorescent probe **NHPO** possessing excellent selectivity and sensitivity toward NAG. Resorufin (**HHPO**) was chosen as the fluorophore due to its long wavelength emission, high fluorescence quantum yield, good water solubility, and efficient tuning of the electrondonating ability *via* alkylation of the 7-hydroxy group. Due to favourable ICT (intramolecular charge transfer) properties, **HHPO** derivatives always display extremely low background, and the fluorescence intensity can be modulated by removing substituents from the hydroxyl group, affording high detection sensitivity for enzyme activity.[11] Furthermore, **NHPO** can be successfully applied to

[a] *Academy of Integrative Medicine, College of Pharmacy, Advanced Institute for Medical Sciences, Dalian Medical University, Lvshun South Road No. 9, Dalian 116044, P. R. China. E-mail: maxc1978@163.com, leifeng@mail.dlut.edu.cn*
[b] *Department of Chemistry, University of Bath, Bath, BA2 7AY, UK. E-mail: t.d.james@bath.ac.uk*
[c] *State Key Laboratory of Fine Chemicals, Dalian University of Technology, Ganjingzi District, Linggong Road No. 2, Dalian 116024, P. R. China*

† Electronic supplementary information (ESI) available. See DOI: 10.1039/c8cc10311a

‡ These authors equally contributed to this work.

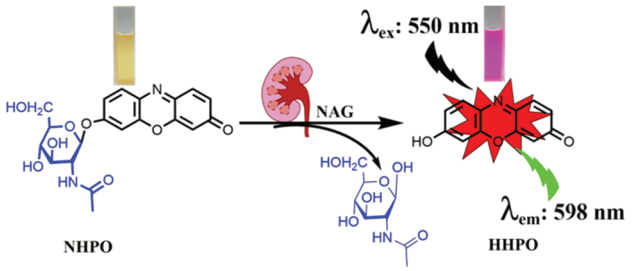

Scheme 1 Chemical structure of **NHPO** and the mechanism of NAG detection.

sense endogenous NAG in a cisplatin-induced kidney injury mice model,[12] and for detecting NAG levels in crude human urine. More importantly, we evaluated the importance of NAG for the early diagnosis of renal injury and proximal tubule cells, as a diagnostic marker that can be used as a practical molecular tool for precision diagnostics in the kidney injury unit.

The fluorescence changes of **NHPO** after incubating with NAG were observed, as shown in Fig. S1 (ESI†) and compared with the negative control (without NAG), a dramatic spectral increase at 575 nm and distinct colour change from light yellow to pink (Scheme 1), were observed after addition of the NAG isoform, in addition a prominent fluorescence emission was also detected at 598 nm. The influence of pH on the fluorescence intensity of **NHPO** and its metabolite **HHPO** was investigated, as shown in Fig. S2 (ESI†), the metabolite **HHPO** has a stable fluorescence intensity from pH 7.0–12.0; additionally, we investigated the effects of pH on the fluorescence of **NHPO** reacting with NAG (Fig. S3, ESI†), the results indicate that **NHPO** has excellent compatibility with NAG under physiological conditions (about pH 7.4 and 37 °C). Furthermore, the fluorescence intensity was linear with increasing NAG enzyme from 0–7 μg mL^{-1}. (Fig. S1c and d, ESI†). Additionally, as shown in Fig. S4 (ESI†), a new chromatographic peak in the HPLC was detected after incubating with NAG which was identified as resorufin (**HHPO**) using HPLC and ESI-MS/MS analysis. These results confirmed that **NHPO** could act as a turn-on fluorescence based probe for the rapid detection of NAG under physiological conditions.

The selectivity of **NHPO** towards NAG was investigated, as shown in Fig. S5 (ESI†), only NAG could trigger the hydrolysis reaction to produce a significant fluorescence emission at 598 nm, other hydrolase enzymes including Ls, α-GLC, Cas, PaK, CE1b, CE1c, CE2, BSA, β-Gla, GLU and β-GLC have no influence on the fluorescence intensity of **NHPO**. Additionally, some common endogenous substance and metal ions including myristic acid, Ser, Trp, Glu, Gly, Cys, Arg, Cys, Lys, Gln, GSH, glucose, Mn^{2+}, Ca^{2+}, Mg^{2+}, Ni^{2+}, Zn^{2+}, Sn^{4+}, K^{+}, Cu^{2+}, Fe^{3+}, Na^{+} and Ba^{2+} all have no effect on the fluorescence intensity of **NHPO**. These results demonstrate that **NHPO** can serve as a highly sensitive and selective probe to detect the bioactivity of NAG in complex biological systems.

In order to reveal the key role of NAG in the diagnosis of kidney injury, a kidney injury model was developed in C57 BL/6 mice using cisplatin. As shown in Fig. 1, after pre-treatment with cisplatin, the urea nitrogen (BUN) and serum creatinine

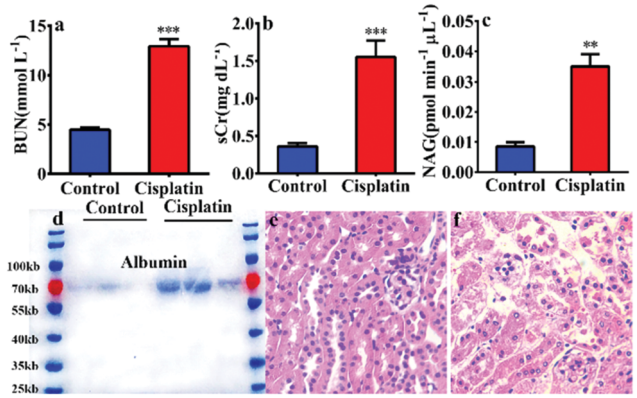

Fig. 1 The activity of (a) BUN, (b) sCr, (c) NAG in the urine of C57BL/6 mice which were treated with cisplatin; (d) the western blot of Albumin in urine; (e and f) the hematoxylin–eosin staining of paraffin section kidney tissues in normal (e) and cisplatin treatment group (f), respectively.

(sCr) levels exhibited a significantly larger increase than that of a control group (BUN 2.9 fold and sCr 4.3 fold). Furthermore, the western blot detected albumin in the mouse urine after treatment with cisplatin (Fig. 1d), all of which suggested that cisplatin could induce significant kidney injury.

Therefore, the NAG activity in urine was assayed using **NHPO**, as shown in Fig. 1c, and the results indicated a significant increase in NAG activity for the urine of the cisplatin-treated group, which was in agreement with the classic evaluation method (BUN and sCr) for kidney injury. Lastly, kidney specimens at a thickness of 10 μm were subjected to hematoxylin–eosin staining and Periodic Acid Schiff (PAS) staining.[13] As shown in Fig. 1e, f and Fig. S6 (ESI†), after treatment with cisplatin, significant kidney damage in the proximal glomerular tubule was observed. All of the above results clearly indicated that NAG could serve as a biomarker in urine for evaluating kidney injury and the function change of kidney proximal glomerular tubule, with **NHPO** acting as a rapid screening tool that could efficiently and sensitively diagnose kidney injury by measuring urine NAG activity.

In order to confirm that **NHPO** can be used to monitor the activity of endogenous NAG in human urine, a correlation study was performed between **NHPO** and the commercial kit, as shown in Fig. 2, NAG activity in 12 human urine samples measured by **NHPO** was consistent with the commercial kit with an r value of 0.98, which also indicates that **NHPO** exhibited excellent selectivity for human NAG. Next, 58 urine samples from renal injury patients (n = 28) and healthy individuals (n = 30) were measured by **NHPO**, NAG activity of patients with varying degrees of kidney injury all exhibited much higher (about 8.2 fold, calculated by the mean values) in urine than that of healthy individuals. These results indicated **NHPO** could serve as a novel tool for clinical diagnosis of human kidney injury using real-time monitoring of the endogenous NAG activity in urine.

Fluorescence imaging of endogenous NAG in living kidney cells was evaluated. Firstly, **NHPO** displayed no cytotoxicity at various concentrations up to 50 μM using a CCK-8 assay. Next, as shown in Fig. S7d (ESI†), after incubation of **NHPO** with HK-2 cells for 1 h at 37 °C, the cells were imaged at an excitation

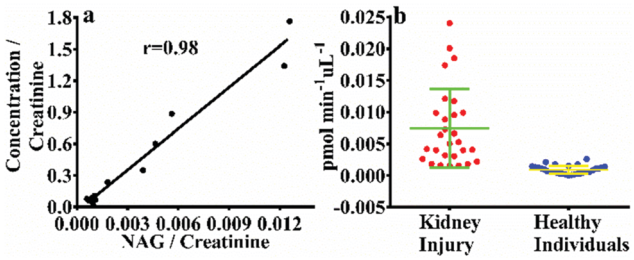

Fig. 2 (a) Correlation analysis (n = 12) between NAG activity measurement by **NHPO** and a commercial NAG assay kit; (b) the NAG activity in several urine samples including healthy individuals and Kidney injury patients. Data points represent the mean value of triplicate experiments for samples that were incubated at 37 °C for 1 h.

wavelength of 561 nm and an obvious signal was detected in the 570–620 nm channel, by contrast, the control cells exhibited no fluorescence (Fig. S7a, ESI†). These results indicated that **NHPO** had good cell permeability and exhibits a hydrolysis process triggered by NAG. Identical fluorescence images were also obtained with NRK-52e (rat renal proximal tubule epithelial cell line) and MCT (mouse renal proximal tubule cell line), respectively (Fig. S8 and S9, ESI†).

Moreover, after knocking down the expression of NAG in HK-2 cells by siNAG transfection, the expression of intracellular NAG was evaluated by western blotting and **NHPO**, respectively. As shown in Fig. 3, the expression of NAG in siNAG transfected HK-2 cells had a sharp decrease; compared to the control group,

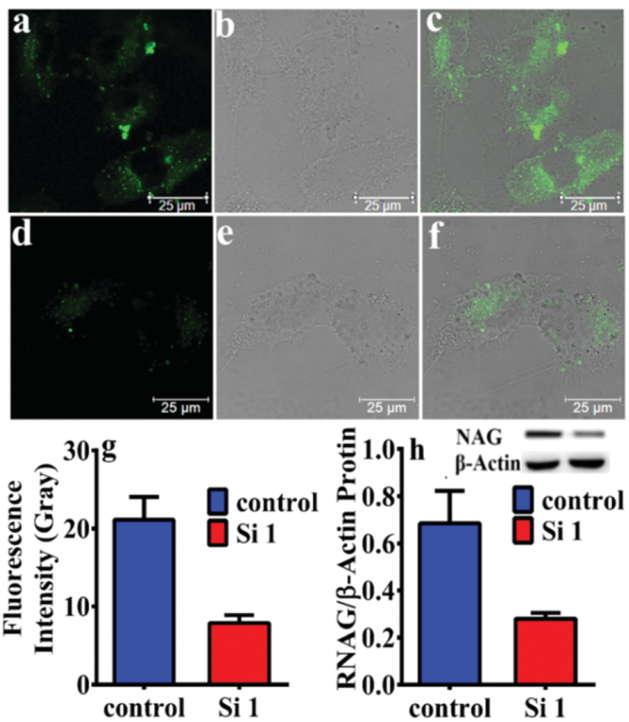

Fig. 3 Fluorescence, bright field and merged image of HK-2 (a–c) and siNAG transfected HK-2 cells (d–f) incubated with **NHPO** (50 μM); (g) the quantitative analysis of the NAG fluorescence intensity in HK-2 and siNAG transfected HK-2 cells; (h) the protein level expression of NAG in HK-2 cells and siNAG transfected HK-2 cells. The scale bar is 25 μm.

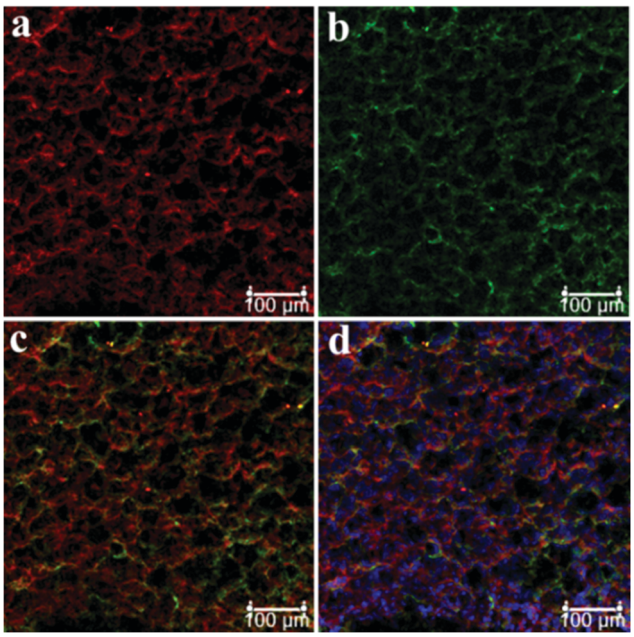

Fig. 4 Fluorescence imaging of NAG (a) and immunofluorescence images of AQP1 (b) for tissue slices of mice kidney, respectively. (c) The merge of NAG and AQP1; (d) merged images of NAG, AQP1 and DAPI for cell nuclei. The scale bar is 100 μm.

the siNAG transfected group exhibited a significantly suppressed fluorescence signal after incubation with **NHPO**. This fluorescence decrease was due to the down-regulation of NAG expression, and further illustrated that **NHPO** is capable of real-time imaging of endogenous NAG in living systems.

Fresh kidney specimens were collected and prepared at a thickness of 10 μm using a cryostat microtome, and subjected to **NHPO** for imaging of NAG, additionally, an immunohistochemical staining with Aquaporin 1 (AQP1, a well-known marker of the proximal tubule) was also performed, as shown in Fig. 4a, the red signal produced by **NHPO** was distributed around the proximal tubule which was consistent with the immuno-histochemical staining by AQP1 (Fig. 4b). A whole tube was observed in the red channel after incubation with **NHPO**, and these results indicate that NAG is specifically expressed in the proximal tubule. Therefore, these findings confirm that **NHPO** can serve as a useful approach for imaging NAG activity in specific kidney units (proximal tubule, PT), and might be used for clinical diagnosis of PT damage in various kidney diseases.

According to the experimental observation mentioned above, we collected and prepared the cells in urine from kidney injury patients and healthy individuals, **NHPO** was used for fluorescence imaging and to diagnose whether proximal tubule injury had occurred in the patients who had kidney disease. In our work, very few cells were detected for the healthy individual (Fig. S10, ESI†); however, a lot of different cell types were detected in the patients' urine. Furthermore, as shown in Fig. 5a–c, no fluorescence background was detected for the cells separated from urine. Interestingly after incubating with **NHPO**, ill-1 displayed no fluorescence response in the fluorescence channel (570–620 nm), however, for ill-2, some cells exhibited a significant fluorescence signal in the

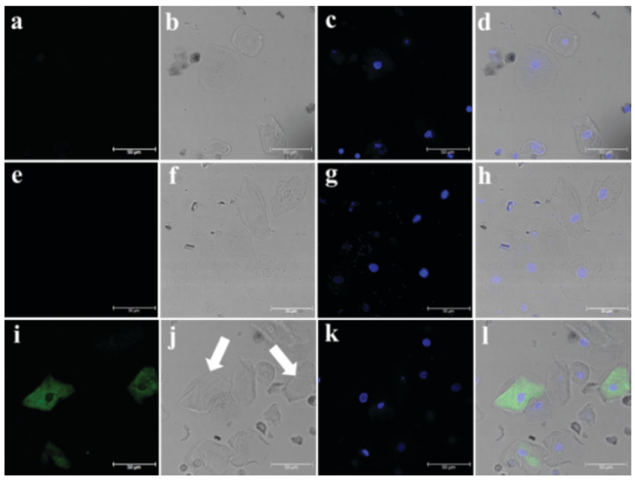

Fig. 5 Fluorescence imaging of cells obtained from the urine of different kidney disease patients after incubation with **NHPO** (50 μM); (a–d) the fluorescence background of cells; (e–h) the imaging of ill-1 patient; (i–l) the imaging of ill-2 patient. The scale bar is 50 μm.

570–620 nm channel. Based on the above results, these cells were confirmed to be proximal tubule epithelial cells. Thus, patient ill-2 might have a proximal tubule injury as part of their kidney disease. These results indicate that **NHPO** could serve as an efficient tool to diagnose and discover PT injury in kidney disease.

In summary, a new enzyme-activated probe **NHPO** exhibiting excellent selectivity and sensitivity for endogenous NAG activity has been developed. The results indicate that **NHPO** could be used for detecting and imaging endogenous NAG in a cisplatin-induced kidney injury mice model with low cytotoxicity and preferred cell penetration. Importantly, using this probe, we revealed the much higher levels of NAG in urine of renal injury patients than from a healthy group, which strongly suggests that NAG could be used as a clinical marker for the early diagnosis of renal injury. Furthermore, **NHPO** could successfully image proximal tubule cells in order to achieve real-time precision diagnostics of the dysfunction of the proximal renal tubules in kidney injury.

The authors thank the National Natural Science Foundation of China (No. 81622047, 81503201 and 21572029), Distinguished Professor of Liaoning Province program and State Key Laboratory of Fine Chemicals (KF1803) for financial support. TDJ wishes to thank the Royal Society for a Wolfson Research Merit Award.

Conflicts of interest

There are no conflicts to declare.

Notes and references

1 (*a*) S. R. Kim, Y. H. Lee, S. G. Lee, E. S. Kang, B. S. Cha, J. H. Kim and B. W. Lee, *Medicine*, 2016, **95**, e4114; (*b*) A. M. Sharifi, B. Zare, M. Keshavarz, M. Rahmani, B. Zaeefy and B. Larijani, *Int. J. Diabetes Dev. Countries*, 2015, 1–6; (*c*) G. H. Tesch, *Clin. Sci.*, 2017, **131**, 2183–2199.

2 (*a*) G. C. Gobe, J. S. Coombes, R. G. Fassett and Z. H. Endre, *Expert Opin. Drug Metab. Toxicol.*, 2015, **11**, 1683–1694; (*b*) N. Goel, J. M. Pullman and M. Coco, *Clin. Kidney J.*, 2014, **7**, 513–517.

3 (*a*) R. Safirstein, J. Winston, D. Moel, S. Dikman and J. Guttenplan, *Int. J. Androl.*, 1987, **10**, 325–346; (*b*) H. Soni, D. Kaminski, R. Gangaraju and A. Adebiyi, *Ren. Fail.*, 2018, **40**, 314–322; (*c*) A. E. Vickers, K. Rose, R. Fisher, M. Saulnier, P. Sahota and P. Bentley, *Toxicol. Pathol.*, 2004, **32**, 577–590.

4 G. Simon, S. Morioka and D. K. Snyder, *Clin. Exp. Hypertens.*, 1984, **6**, 879–896.

5 (*a*) M. Abdelsalam, E. Elmorsy, H. Abdelwahab, O. Algohary, M. Naguib, A. A. El Wahab, A. Eldeeb, E. Eltoraby, A. Abdelsalam, A. Sabry, M. El-Metwally, M. Akl, N. Anber, M. El Sayed Zaki, F. Almutairi and T. Mansour, *BMC Nephrol.*, 2018, **19**, 219; (*b*) P. Devarajan, *Curr. Opin. Pediatr.*, 2011, **23**, 194–200; (*c*) C. L. Edelstein, *Biomarkers of Kidney Disease*, 2nd edn, 2017, ch. 6, pp. 241–315.

6 (*a*) R. L. Sherman, D. E. Drayer, B. R. Leyland-Jones and M. M. Reidenberg, *Arch. Intern. Med.*, 1983, **143**, 1183–1185; (*b*) M. Nishida, H. Kawakatsu, H. Komatsu, K. Ishiwari, M. Tamai, K. Tsunamoto, Y. Kasubuchi and T. Sawada, *Acta Paediatr. Jpn.*, 1998, **40**, 424–426.

7 D. N. Patel and K. Kalia, *Int. J. Diabetes Dev. Countries*, 2015, **35**, 1–9.

8 A. Noto, Y. Ogawa, S. Mori, M. Yoshioka, T. Kitakaze, T. Hori, M. Nakamura and T. Miyake, *Clin. Chem.*, 1983, **29**, 1713–1716.

9 (*a*) L. Feng, Y. Yang, X. Huo, X. Tian, Y. Feng, H. Yuan, L. Zhao, C. Wang, P. Chu, F. Long, W. Wang and X. Ma, *ACS Sens.*, 2018, **3**, 1727–1734; (*b*) X. Han, X. Song, F. Yu and L. Chen, *Chem. Sci.*, 2017, **8**, 6991–7002; (*c*) X. Huo, X. Tian, Y. Li, L. Feng, Y. Cui, C. Wang, J. Cui, C. Sun, K. Liu and X. Ma, *Sens. Actuators, B*, 2018, **262**, 508–515; (*d*) Y. Jin, X. Tian, L. Jin, Y. Cui, T. Liu, Z. Yu, X. Huo, J. Cui, C. Sun, C. Wang, J. Ning, B. Zhang, L. Feng and X. Ma, *Anal. Chem.*, 2018, **90**, 3276–3283; (*e*) H. W. Liu, L. Chen, C. Xu, Z. Li, H. Zhang, X. B. Zhang and W. Tan, *Chem. Soc. Rev.*, 2018, **47**, 7140–7180; (*f*) J. Ning, T. Liu, P. Dong, W. Wang, G. Ge, B. Wang, Z. Yu, L. Shi, X. Tian, X. Huo, L. Feng, C. Wang, C. Sun, J. N. Cui, T. D. James and X. Ma, *J. Am. Chem. Soc.*, 2018, DOI: 10.1021/jacs.8b12136; (*g*) J. Zhang, X. Chai, X. P. He, H. J. Kim, J. Yoon and H. Tian, *Chem. Soc. Rev.*, 2018, DOI: 10.1039/c7cs00907k.

10 (*a*) E. J. Kim, D. O. Kang, D. C. Love and J. A. Hanover, *Carbohydr. Res.*, 2006, **341**, 971–982; (*b*) H. Matsuzaki, M. Kamiya, R. J. Iwatate, D. Asanuma, T. Watanabe and Y. Urano, *Bioconjugate Chem.*, 2016, **27**, 973–981.

11 (*a*) A. E. Albers, K. A. Rawls and C. J. Chang, *Chem. Commun.*, 2007, 4647–4649; (*b*) X. Wu, W. Shi, X. Li and H. Ma, *Angew. Chem., Int. Ed.*, 2017, **56**, 15319–15323.

12 (*a*) R. Galgamuwa, K. Hardy, J. E. Dahlstrom, A. C. Blackburn, E. Wium, M. Rooke, J. Y. Cappello, P. Tummala, H. R. Patel, A. Chuah, L. Tian, L. McMorrow, P. G. Board and A. Theodoratos, *J. Am. Soc. Nephrol.*, 2016, **27**, 3331–3344; (*b*) Y. Miyasato, T. Yoshizawa, Y. Sato, T. Nakagawa, Y. Miyasato, Y. Kakizoe, T. Kuwabara, M. Adachi, A. Ianni and T. Braun, *Sci. Rep.*, 2018, **8**, 5927.

13 (*a*) H. Pan, K. Shen, X. Wang, H. Meng, C. Wang and B. Jin, *PLoS One*, 2014, **9**, e86057; (*b*) F. Li, Y. Yao, H. Huang, H. Hao and M. Ying, *Int. Immunopharmacol.*, 2018, **61**, 277–282.

